Regular Article

Chitosan-Acrylic Polymeric Nanoparticles with Dynamic Covalent Bonds. Synthesis and Stimuli Behavior

Herman Palacio,[a] Felipe Otálvaro,[b] Luis Fernando Giraldo,[c] Gilles Ponchel,[d] and Freimar Segura-Sánchez*,[a]

[a] *Grupo de Investigación BIOPOLIMER, Facultad de Ciencias Farmacéuticas y Alimentarias, Universidad de Antioquia; Carrera 50 A # 63–85, Medellín, Colombia:* [b] *Grupo de Investigación Síntesis y Biosíntesis de Metabolitos Naturales, Instituto de Química, Universidad de Antioquia; Calle 67 No. 53–108, Medellín, Colombia:* [c] *Laboratorio de Investigación en Polímeros, Instituto de Química, Universidad de Antioquia; Calle 67 No. 53–108, Medellín, Colombia: and* [d] *Institut Galien Paris-Sud UMR CNRS 8612; 5 rue J-B. Clément, 92296 Châtenay-Malabry, France.*
Received August 3, 2017; accepted October 4, 2017; advance publication released online October 12, 2017

Drug delivery represents one of the most important research fields within the pharmaceutical industry. Different strategies are reported every day in a dynamic search for carriers with the ability to transport drugs across the body, avoiding or decreasing toxic issues and improving therapeutic activity. One of the most interesting strategies currently under research is the development of drug delivery systems sensitive to different stimuli, due to the high potential attributed to the selective delivery of the payload. In this work, a stimuli-sensitive nanocarrier was built with a bifunctional acrylic polymer, linked by imine and disulfide bonds to thiolate chitosan, the latter being a biopolymer widely known in the field of tissue engineering and drug delivery by its biodegradability and biocompatibility. These polymer nanoparticles were exposed to different changes in pH and redox potential, which are environments commonly found inside cancer cells. The results proof the ability of the nanoparticles to keep the original structure when either changes in pH or redox potential were applied individually. However, when both stimuli were applied simultaneously, a disassembly of the nanoparticles was evident. These special characteristics make these nanoparticles suitable nanocarriers with potential for the selective delivery of anticancer drugs.

Key words polymeric nanoparticle; stimuli-sensitive nanoparticle; drug delivery; acrylic monomer; thiolated chitosan

The process of vectoring and encapsulation of existing drugs is one of the exploration fields that has attracted more attention in the pharmaceutical technology area.[1)] Many encapsulation systems have been proposed as vector agents such as liposomes,[2)] microspheres,[3,4)] polymeric micelles[5,6)] and other types of nanoparticles.[7–10)] However, most of them lack selectivity in the delivery of the payload. In order to overcome this problem, histological and molecular investigations of cancer cells have been done with the aim to make a general characterization of these cells.[11)] Some of the most important findings indicate that cancerous tissues are highly heterogeneous.[12)] However, there are a number of common characteristics in different types of cancer cells and tumoral tissues which differentiate them from healthy tissues, extracellular pH being one of them. Normal tissues usually present an extracellular pH of 7.4 whereas carcinogenic tissues reach values of 6.5 mainly as a consequence of irregular angiogenesis in fast-growing tumors, which causes a rapid deficit of both nutrients and oxygen with a consequent shift towards glycolytic metabolism which leads to an increased production of acidic metabolites.[13)] At the intracellular level, the pH of endosomes of cancer cells fluctuates around 5.0 while in normal ones is around 6.0. Other differential parameters noted are the almost 100-fold higher concentration of glutathione (GSH) and the higher temperature registered in tumor mass and cancer cells.[14–16)]

Thus, the development of drug delivery systems that take advantages of such differential properties between healthy and cancerous cells is highly desirable. Some researchers have developed pH stimuli sensitive nanocarriers based on ionic bonds[17)] however, those systems are no suitable when a soft stimulus is applied.

Other interesting tool that has been used in the development of stimuli sensitive drug delivery systems relies on the concept of dynamic covalent bonds, which are sensitive to weak stimuli. The term 'dynamic covalent bond' describes any covalent chemical bond which possesses the capacity to be formed or broken as a function of the system conditions.[18)] Some examples can be found in imine, hydrazine, disulfide, oxime and acetal/ketal bonds.[19)] The imines, for example, result as the interaction of primary amines and aldehydes and are sensitive to changes in pH.[20)] Disulfides are the product of the reaction between thiols and are sensitive to reductant species.[21)] In principle, nanocarriers that include dynamic covalent bonds should be strong enough to reach the target tissue without significant changes in their structure and then respond to the specific environment conditions allowing the release of the drug payload.

In 2012, Jackson and Fulton provided one such example of a polymer nanocarrier based on two synthetic polymeric units structured with acrylamide derivative monomers.[22)] This vector has the ability to release the payload when it is exposed to environments with pH under 5.5 and high redox potential. The fact that the carrier must be exposed to two different stimuli at the same time to release the payload represents a tremendous advantage in terms of selectivity of drug release.

Several materials have been reported for the design and production of drug vectorization systems, from inorganic ma-

* To whom correspondence should be addressed. e-mail: freimar.segura@udea.edu.co

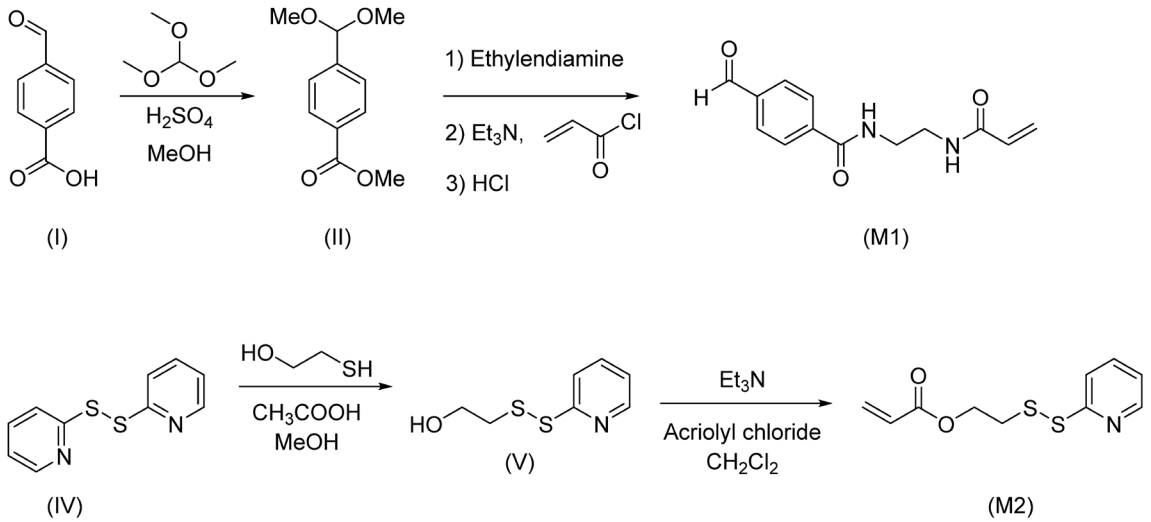

Chart 1. Synthesis of *N*-Ethylacrylamide-2-(4-formylbenzamide) Monomer (**M1**) and Pyridyldisulfide Ethylacrylate Monomer (**M2**)

terials to materials of biological origin.[10,23–25] In this regard, biopolymers like chitosan seems to be an attractive choice, not only for its bioavailability, biocompatibility and biodegradability propierties,[26–33] but also its reported antiseptic and muco-adhesiveness characteristics.[34–36] As a matter of fact, this polymer has been used in a wide variety of systems where it has been successfully combined with synthetic polymers having as a result the improvement of various mechanical and biological properties.[37,38]

In line with the work of Jackson and Fulton,[22] we wish to report here the synthesis of a a new stimuli-sensitive nanostructured system in which one of the polymeric acrylamide subunits is replaced by thiolate chitosan of semisynthetic origin in order to have a potentially biocompatible material as part of the structural base of the nanoparticles. In addition, the material response towards pH and redox potential stimuli is reported.

Experimental

General Information IR spectra were obtained from a PerkinElmer, Inc. Spectrometer (Spectrum Two, FT-IR) by attenuated total reflectance (ATR) (16 scans). Routine ^{1}H- and ^{13}C-NMR spectra of acrylic monomers and polymers were run on a Bruker AVANCE Spectrometer operating at 300 MHz, correlation spectroscopy (COSY), heteronuclear multiple bond connectivity (HMBC), heteronuclear single quantum coherence (HSQC) and nuclear Overhauser effect spectroscopy (NOESY) were run on a Bruker DPX 400 NMR spectrometer. All spectra of chitosan and derivatives were run on a Bruker AVANCE III 600 MHz NMR spectrometer with 5 mm TCI probe. Tetramethylsilane (TMS) was used as internal standard. A microtitration plate reader (BIO RAD IMark) was used to measure the absorption. Particle size and *Z* potential were analyzed by Dynamic Light Scattering (DLS) in a Malvern Zetasizer NanoZS90. Nanoparticles micrographs were recorded *via* Transmission Electron Microscopy (TEM) using a Tecnai G2 F20 TEM. Differential Scanning Calorimetry analyses was run on a TA DSC Q20 and TA DSC Q100; the sample was heated under nitrogen from room temperature up to 200°C at a rate of 20°C/min and then cooled to −30°C at a rate of 10°C/min, finally was heated again up to 200°C at a rate of 20°C/min. The molecular weight of chitosan was determined using a MicroTube μ-Ubbelohde: type 53710/I n° 1016187 Schott Geräte Capillary Viscometer (K=0.01022 mm^3/s) equipped with an AVS400 detection System. Analyses were carried out using a solution of acetic acid 0.1 M and NaCl 0.2 M as a solvent at 25°C. Molecular weight of acrylic polymers was determined by Size Exclusion Chromatography (SEC) using two columns from Polymer Laboratories (PL-gel MIXED-D; 300×7.5 mm; bead diameter, 5 μm; linear part, 400–4×105 g/mol) and a Differential Refractive Index Detector (Spectrasystem RI-150 from Thermo Electron Corp.), using chloroform ($CHCl_3$) as eluent, and toluene as a flowrate marker at a flow of 1 mL/min. Samples were filtered with a 0.2 μm polytetrafluoroethylene (PTFE) filter before analysis. The calibration curve was based on poly(methyl methacrylate) (PMMA) standards from Polymer Laboratories. The samples were Freeze-dry in a BenchTop Pro with Omnitronics VirTis SP SCIENTIFIC freeze drier.

Synthesis of Acrylic Monomers

General Procedure for the Preparation of the Acrylic Monomer with Aldehyde Functionality (**M1**)

Synthesis of Methyl-4-(dimethoxymethyl)benzoate

Methyl-4-(dimethoxymethyl)benzoate (**II**) was synthesized following a procedure described in the literature[39] with some modifications (higher amount of sulfuric acid and the reprocess of the sample). The reaction is shown in the Chart 1. Briefly, 4-carboxybenzaldehyde (**I**) (770.0 mg), trimethylorthoformate (5.0 mL), concentrated H_2SO_4 (25 drops) and methanol (5.0 mL) were mixed and heated up to 75°C in a reflux system for 48 h. The reaction mixture was transferred to a separating funnel with saturated $NaHCO_3$ (aq) (5.0 mL) and extracted with CH_2Cl_2 (3×10.0 mL). The organic extracts were combined and dried over Na_2SO_4, filtered, and evaporated to dryness in order to obtain a crude yellow liquid. The reaction crude was again refluxed with a solution of trimethylorthoformate (5.0 mL) and concentrated H_2SO_4 (25 drops) in methanol (5.0 mL) and extracted as before to afford a pale yellow liquid. Yield 95%. ^{1}H-NMR (300 MHz, $CDCl_3$) δ: 8.04 (d, J=8.3 Hz, 2H), 7.53 (d, J=8.1 Hz, 2H), 5.44 (s, 1H), 3.92 (s, 3H), 3.33 (s, 6H). ^{13}C-NMR (75 MHz, $CDCl_3$) δ: 166.99 (s), 143.07 (s), 130.35 (s), 129.65 (s), 126.93 (s), 102.50 (s), 52.78 (s), 52.23

(s). FT-IR (wavenumber, cm^{-1}) 2995, 2954, 2902, 2832, 1724, 1577, 1509, 1438, 1280.

Synthesis of *N*-Ethylacrylamide-2-(4-(dimethoxymethyl)-benzamide)

Methyl-4-(dimethoxymethyl)benzoate (700.0 mg) and 1,2-diaminoethane (10.0 mL) were mixed and heated up to 80°C for 24 h and then evaporated to dryness under vacuum. The yellow solid obtained was dissolved in dry CH_2Cl_2 (20.0 mL) and triethylamine (Et_3N) (20.0 mL) was added. The solution was cooled to 0°C in an ice bath. Acryloyl chloride (520.0 mg) in CH_2Cl_2 (10.0 mL) was added dropwise for a period of 30 min. The reaction was stirred overnight at room temperature and then transferred to a separating funnel with saturated $NaHCO_3$ (aq) (30.0 mL). The aqueous layer was extracted with CH_2Cl_2 (3×30.0 mL). The organic extracts were combined and dried over Na_2SO_4, filtered, and evaporated to dryness under vacuum to afford a crude solid, which was purified by column chromatography using silica gel as stationary phase and a mixture of CH_2Cl_2–MeOH (90 : 10 v/v) as eluent to obtain a white solid. ^{1}H-NMR (300 MHz, $CDCl_3$) δ: 7.81 (d, J=8.3 Hz, 1H), 7.50 (d, J=8.2 Hz, 1H), 6.27 (dd, J=17.0, 1.6 Hz, 1H), 6.13 (dd, J=17.0, 10.0 Hz, 1H), 5.63 (dd, J=10.0, 1.6 Hz, 1H), 5.41 (s, 1H), 3.59 (s, 2H), 3.31 (s, 3H). ^{13}C-NMR (75 MHz, $CDCl_3$) δ: 168.23 (s), 167.17 (s), 141.59 (s), 133.99 (s), 130.61 (s), 127.00 (s), 126.78 (s), 102.43 (s), 52.69 (s), 41.10 (s), 39.98 (s). FT-IR (wavenumber cm^{-1}) 3300, 3072, 2986, 2942, 2903, 2831, 1643, 1544, 1505, 1436, 1250.

Synthesis of *N*-Ethylacrylamide-2-(4-formylbenzamide) (**M1**)

A solution of *N*-ethylacrylamide-2-(4-(dimethoxymethyl)-benzamide) (500.0 mg) in 1.0 M HCl(aq) (5 mL) was stirred at room temperature for 2 h and then neutralized with saturated $NaHCO_3$(aq) (30.0 mL). The aqueous layer was extracted with EtOAc (50.0 mL) 3 times and the organic extracts were combined and dried over $MgSO_4$, filtered, and evaporated to dryness under vacuum to obtain a pale yellow solid which was purified by column chromatography using silica gel as stationary phase and a mixture of CH_2Cl_2–MeOH (96 : 4 v/v) as eluent to afford a white solid. ^{1}H-NMR (300 MHz, dimethyl sulfoxide (DMSO)) δ: 10.14 (s, 1H), 8.84 (s, 1H), 8.32 (s, 1H), 8.13–8.02 (m, 4H), 6.27 (dd, J=17.1, 9.8 Hz, 1H), 6.15 (dd, J=17.1, 2.3 Hz, 1H), 5.65 (dd, J=9.8, 2.3 Hz, 1H), 3.41 (dd, J=11.0, 6.1 Hz, 4H). ^{13}C-NMR (101 MHz, DMSO) δ: 192.87 (s), 165.56 (s), 164.90 (s), 139.49 (s), 137.73 (s), 131.77 (s), 129.35 (s), 127.92 (s), 125.07 (s), 38.15 (s). FT-IR (wavenumber, cm^{-1}) 3270, 3094, 2986, 2940, 2820, 2783, 2773, 1702, 1643, 1547, 1503, 1447, 1382. The final product was also analyzed by COSY, HSQC, HMBC and NOESY NMR spectroscopy as supplementary characterization and is available in the Supplementary Materials from S7 to S10.

General Procedure for the Preparation of the Acrylic Monomer with Disulfide Functionality (**M2**)

Synthesis of Hydroxyethyl Pyridyldisulfide

Hydroxyethyl pyridyldisulfide (HPDS) (**V**) was synthesized according to the literature.[40] The reaction is shown in the Chart 1. Briefly, dithiodipyridine (DTDP) (**IV**) (5.0 g) was dissolved in methanol (25.0 mL) and glacial acetic acid (350 μL) was then added. After that, a solution of mercaptoethanol (530 μL) in methanol (5.0 mL) was added dropwise at room temperature during 30 min under continuous stirring. Once the addition was over, the reaction mixture was stirred at room temperature for 4 h. The stirring was stopped and the solvent was evaporated to get the crude product as yellow oil. The crude product was then purified by column chromatography using silica gel as stationary phase and a mixture of ethyl acetate–cyclohexane (15 : 85, v/v) as eluent. The purification was monitored by TLC, the fraction with Rf=0.33 was collected and the solvent was removed to get the desired product as pale yellow oil. Yield: 68%. ^{1}H-NMR (300 MHz, $CDCl_3$) δ: 8.50 (d, J=4.1 Hz, 1H), 7.57 (td, J=7.7, 1.8 Hz, 1H), 7.40 (d, J=8.0 Hz, 1H), 7.14 (dd, J=6.9, 5.5 Hz, 1H), 3.82–3.77 (m, 2H), 2.98–2.91 (m, 2H).

Synthesis of Pyridyldisulfide Ethylacrylate (**M2**)[41]

To a solution of HPDS (V) (1.5 g) in dry CH_2Cl_2 (20.0 mL), Et_3N (1.0 g) was added and the mixture was cooled in an ice bath. After that, a solution of acryloyl chloride (1.0 g) in dry CH_2Cl_2 (10.0 mL) was added during 30 min. The mixture was stirred at room temperature for 12 h. The stirring was stopped and the solid was removed by filtration. The obtained product was mixed with water (20.0 mL). The aqueous layer was extracted with CH_2Cl_2 (3×30.0 mL). The organic extracts were combined and dried over Na_2SO_4, filtered, and evaporated to dryness under vacuum to afford a crude product as brown oil, which was purified by column chromatography using silica gel as stationary phase and a mixture of ethyl acetate–cyclohexane (25 : 75, v/v) as eluent to afford a pale yellow oil. Yield: 78 wt%. The reaction is shown in the Chart 1. ^{1}H-NMR (300 MHz, $CDCl_3$) δ: 8.52–8.40 (m, 1H), 7.72–7.57 (m, 2H), 7.12–7.05 (m, 1H), 6.40 (dd, J=17.3, 1.4 Hz, 1H), 6.09 (dd, J=17.3, 10.4 Hz, 1H), 5.83 (dd, J=10.4, 1.4 Hz, 1H), 4.41 (t, J=6.4 Hz, 2H), 3.08 (t, J=6.4 Hz, 2H). ^{13}C-NMR (101 MHz, $CDCl_3$) δ: 165.93 (s), 159.82 (s), 149.88 (s), 137.14 (s), 131.40 (s), 128.16 (s), 120.98 (s), 119.96 (s), 62.42 (s), 37.51 (s). The final product was also analyzed by COSY, HSQC, HMBC and NOESY NMR spectroscopy as supplementary characterization and is available in the Supplementary Materials from S14 to S17.

Synthesis of Bi-functionalized Acrylic Copolymer (P1) The copolymer P1 was made by RAFT polymerization following a procedure described in the literature.[22] *S*-1-Dodecyl-*S*′-(α,α-dimethyl-α″-acetic acid)trithiocarbonate (DDMAT) (20.8 mg) and AIBN (1.9 mg) were added to a small Schlenk tube. *N*,*N*′-Dimethylacrylamide (910 mg, 9,18 mmol), *N*-ethylacrylamide-2-(4-formylbenzamide) (281.0 mg, 1,14 mmol), and 2-pyridyl disulfide ethylacrylate (276,0 mg, 1,14 mmol) were then added followed by *N*,*N*-dimethylformamide (DMF) (4 mL). The reaction mixture was degassed by 5 cycles of freeze-vacuum-thaw and then it was bubbled for 30 min with argon. The vessel was backfilled with argon and allowed to warm to room temperature. The reaction mixture was then placed in an oil bath at 70°C with constant magnetic stirring, and the polymerization was quenched after 21 h with liquid nitrogen. The reaction mixture was dissolved in a minimal amount of tetrahydrofuran (THF) and added dropwise to a large excess of ice-cold diethyl ether. The solid polymer was then isolated by filtration, and the precipitation was repeated once before drying under high vacuum. Polymer **P1** was obtained as a pale yellow solid. A schematic reaction can be seen in Chart 2. ^{1}H-NMR (400 MHz, $CDCl_3$) δ: 10.06 (s), 8.44 (s), 8.11 (s), 7.91 (s), 7.66 (s), 7.09 (s), 4.30 (s), 3.72 (s), 3.09 (s), 2.87 (s), 2.62 (s), 2.14 (s), 1.83 (s), 1.61 (s), 1.23 (s), 0.85 (s). P1 was also analyzed by size exclusion chromatography (SEC) to evaluate the molecular weight and differential scanning calo-

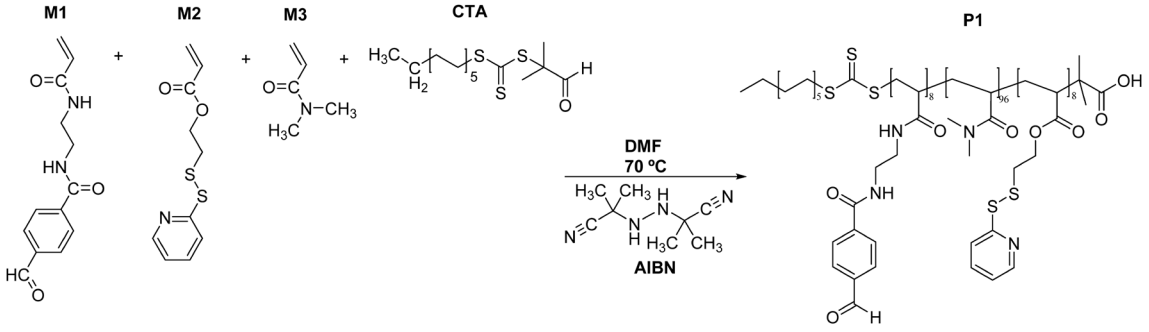

Chart 2. Synthesis of Acrylic Copolymer (**P1**) by RAFT

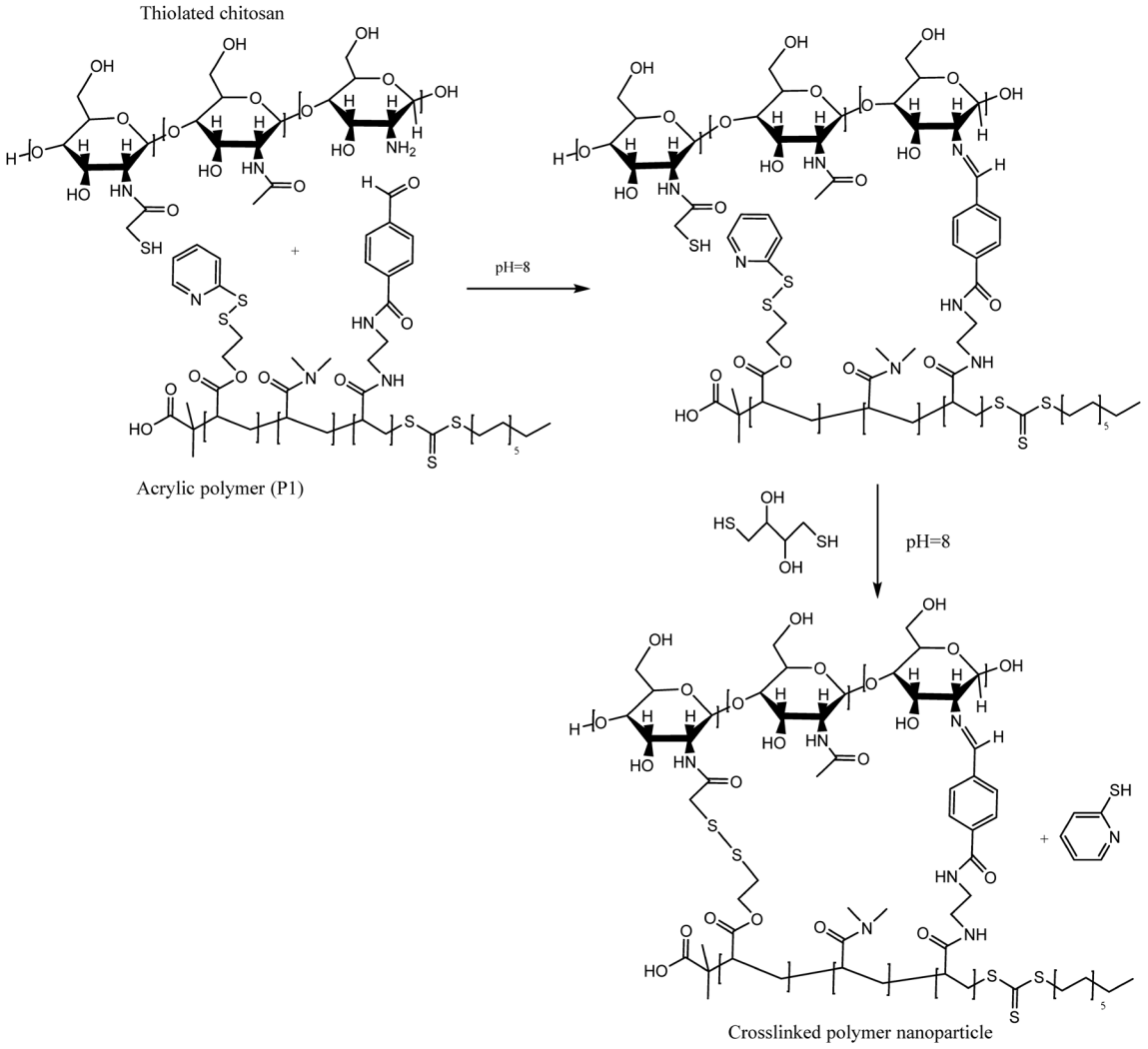

Chart 3. Schematic Representation of Cross-Linking Process between Thiolated Chitosan and Acrylic Polymer (**P1**) *via* Dynamic Covalent Bonds

rimetry (DSC) to evaluate the thermal behavior of the final copolymer.

Preparation of Low Molecular Weight Chitosan (Hydrolyzed Chitosan) Depolymerization of high molecular weight chitosan using the nitrous acid hydrolysis method was made according to literature[42] to afford a low molecular weight polymer. In general, a 2% (w/v) solution of chitosan in acetic acid (6% (v/v)) was prepared. Then a solution of sodium nitrite 0.13 M (25.0 mL) was added dropwise in about 20 min and stirred for two hours at room temperature to get the desired viscosity level. The depolymerized chitosan was then neutralized by a 4.0 M solution of NaOH. The precipitate chitosan was then isolated by filtration and washed thrice with acetone. The solid product was dissolved in a minimal amount of acetic acid solution and dialyzed using dialysis tubing (molecular weight cutoff 3500 Da) against alkaline water pH 8.0. The polymer solution was recovered and freeze-dried. The molecular weight was determined by viscosimetry using chitosan solutions with different concentrations and Mark–Houwink equation.[43]

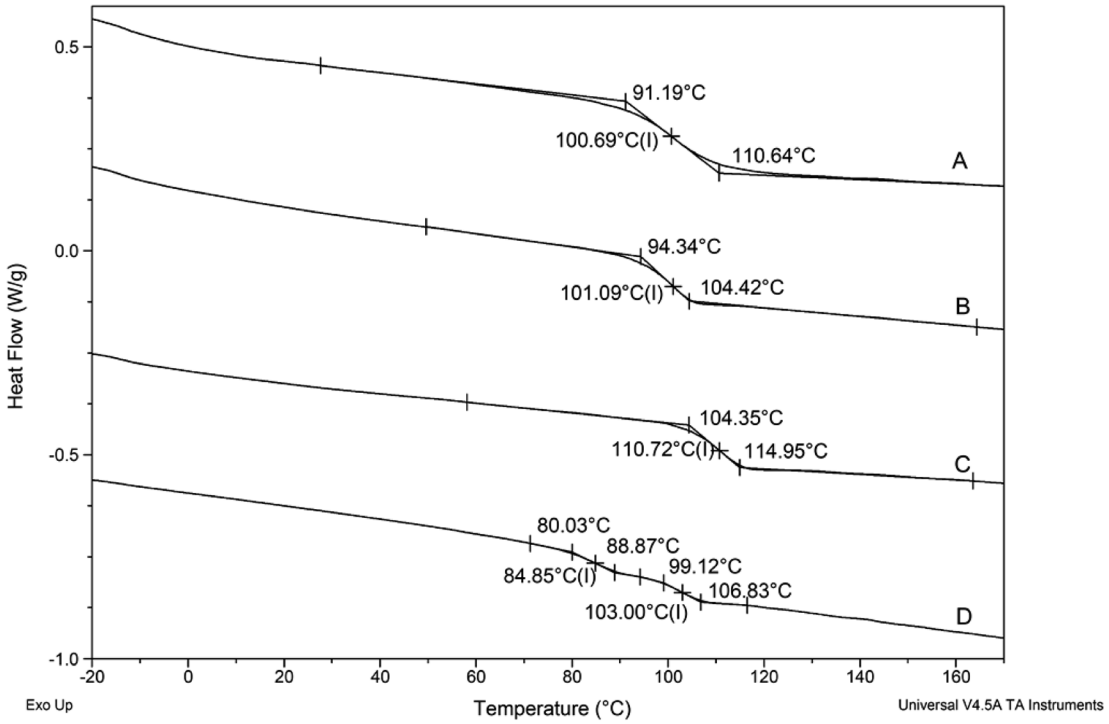

Fig. 1. DSC Profiles of Different Polymers

(A) Homopolymer of monomer **M1**, (B) copolymer of monomers M1, M2 and M3 (**P1**), (C) homopolymer of monomer **M3**, (D) copolymer of monomers **M2** and **M3**.

Functionalization of Hydrolyzed Chitosan One gram of hydrolyzed chitosan was dispersed in water (50.0 mL) by stirring, then HCl 1 M (2.0 mL) was added and the concentration adjusted with water to obtain a 1% (w/v) polymer solution. The mixture was kept under magnetic stirring for 2 h to guarantee the complete dissolution of the polymer. Afterwards, thioglycolic acid (640 μL) was added under continuous stirring. 1-Ethyl-3-(3-dimethylaminopropyl)carbodiimide (EDC) (3.5 g) addition follows and the pH adjusted to 5.5 using HCl (0.1 M). The reaction mixture was kept for 3 h at room temperature under stirring. To eliminate unbound reagents, the resulting functionalized polymer was dialyzed using dialysis tubing (molecular weight cutoff 3500 Da) first, against HCl 5.0 mM, then twice against HCl 5.0 mM containing NaCl (1% (w/v)), and finally twice against HCl 1 mM. Controls were prepared in the same way but omitting EDC during the coupling reaction. Finally, the aqueous polymer solution was freeze-dried at −50°C (0.01 mbar) and stored at 4°C until further use.

Determination of Degree of Functionalization in Chitosan The amount of modified chitosan was evaluated with Ellman's reagent.[44] Briefly, functionalized polymer (0.5 mg) was dissolved in water (250 μL). Then phosphate buffer [pH 8.0, 0.5 M (250 μL) and Ellman's reagent (500 μL) (3 mg of 5,5-dithiobis(2-nitrobenzoic acid) dissolved in 10.0 mL of 0.5 M phosphate buffer pH 8.0], were added. The reaction was allowed to proceed for 3 h at room temperature. Afterwards, the precipitated polymer was removed by centrifugation (24000×$\boldsymbol{g}$; 5 min) and 300 μL of the supernatant fluid was transferred to a microtitration plate. The absorbance was immediately measured at a wavelength of 450 nm with a microtitration plate reader. The amount of thiol moieties was calculated from a standard curve obtained with cysteine HCl. Further analyses were done by NMR to confirm functionalization.

Preparation of Cross-Linked Nanoparticles Initially, two solutions were prepared: thiolated chitosan (25.0 mg) was dissolved in water (5 mL) and copolymer P1 (25.0 mg) was dissolved in THF (1 mL). These two solutions were combined under rapid stirring. Afterwards, the pH was adjusted to 8.0 with NaOH 0.1 M and the reaction was stirred for 24 h to allow the organic solvent to evaporate. Then a solution of dithiothreitol (30.0 mg in 65.0 mL of water pH 8.0) was added, and the reaction was left to stir at room temperature for 16 h. To eliminate low molecular weight products of the reaction and the unreacted reagents, the mixture was dialyzed using dialysis tubing (molecular weight cutoff 3500 Da) twice against water pH 8.0. Finally the reaction mixture (nanoparticles) was analyzed by DLS and TEM, and freeze dried to be analyzed by DSC. A schematic illustration of the cross-linking process between the polymers can be seen in Chart 3.

Functionalization of Nanoparticles To a sample of cross-linked nanoparticles in water (0.5 wt%, pH 5.5, 3 mL) NHS end-functionalized poly(ethylene glycol) (PEG) 5000 (6.0 mg) under magnetic stirring was added (PG1-SC-5k NANOCS). The reaction was left to stir at room temperature for 24 h. To eliminate unreacted PEG, the mixture was dialyzed using dialysis tubing (molecular weight cutoff 8000 kDa) twice against water pH 8.0. Finally the nanoparticles were analyzed by DLS.

Evaluation of Nanoparticle Sensibility to pH and Redox Potential Stimuli Four samples of cross-linked nanoparticles were exposed to four different environment conditions: a) acid pH (5.5), b) higher redox potential with tris(2-carboxyethyl)phosphine (TCEP), c) acid pH (5.5) and higher redox potential (with TCEP), and d) neither acid pH nor higher redox potential (pH 8.0, without TCEP) as control. For a) the pH of a sample of cross-linked nanoparticles (pH 8.0, 6 mL) was adjusted to 5.5 with small aliquots of HCl 0.1 M. The reaction was left to re-equilibrate at room temperature for 16 h. For b) a sample of cross-linked nanoparticles (pH 8.0, 6.0 mL)

			Size (d.nm):	% Intensity:	St Dev (d.n...
Z-Average (d.nm):	86,58	Peak 1:	103,7	100,0	42,35
PdI:	0,158	Peak 2:	0,000	0,0	0,000
Intercept:	0,966	Peak 3:	0,000	0,0	0,000
Result quality :	Good				

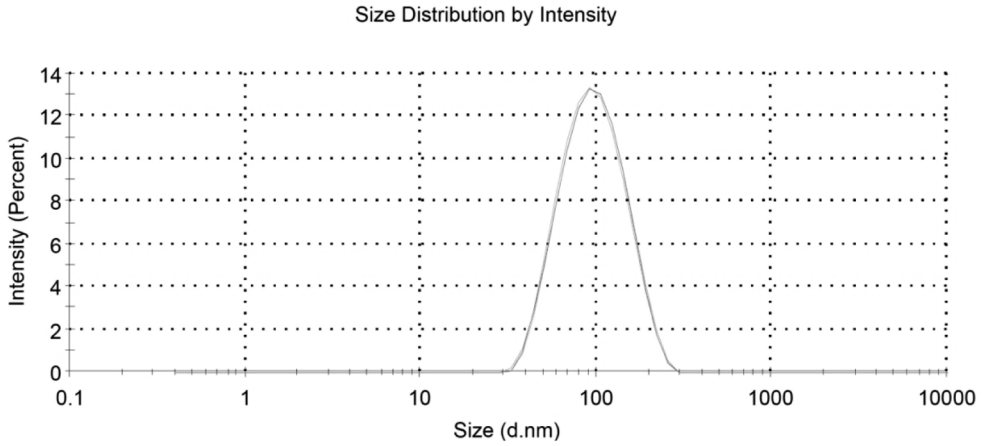

Fig. 2. Size Distribution of Cross-Linked Polymer Nanoparticles and Polydispersity Index Measured by Dynamic Light Scattering

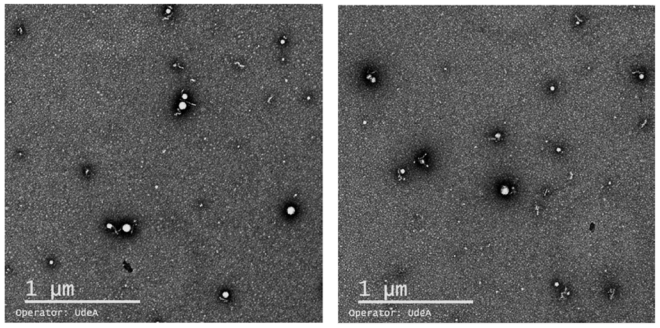

Fig. 3. TEM Photography of Cross-Linked Polymer Nanoparticles

was treated with tris(2-carboxyethyl)phosphine (TCEP) (1 mg) (approximately 5 eq per each disulfide bond) and the reaction was left to stir at room temperature for 16 h. For c) a sample of cross-linked nanoparticles was exposed to the effect of both stimuli, change of pH and reductant agent as described above and left to react for 16 h and for d) a sample of cross-linked nanoparticles was left to stir at room temperature for 16 h without modifications of original conditions. Finally the samples were analyzed by DLS. Furthermore, the structural changes of the nanoparticles by the effect of the change in pH were also followed by ^{1}H-NMR.

Results and Discussion

Synthesis of Acrylic Monomers The first part of the work focused in the synthesis of acrylic monomers with certain functional groups as starting material to build bifunctional polymers. The synthesis of *N*-ethylacrylamide-2-(4-formylbenzamide) (**M1**) was accomplished in four steps (Chart 1) starting from 4-formylbenzoic acid (**I**). Thus, treatment of 4-formylbenzoic acid (**I**) with trimethylorthoformate afforded the corresponding methyl benzoate acetal (**II**). Monoacylation of ethylendiamine with this protected benzoate was followed by the introduction of the acrylate moiety by means of acylation of the free amino group with acryloyl chloride. Hydrolysis of the acetal afforded **M1** in a 95% global yield.

The synthesis of monomer **M2**, involved the substitution of dithiodipyridine (IV) with mercaptoethanol followed by acylation with acryloyl chloride to afford 2-(pyridin-2-yldisulfaneyl)ethyl acrylate (**M2**) in a 68% global yield.

Mercaptoethanol was chosen instead of the usual cysteamine in order to decrease the synthetic cost at the expense of changing a stronger amide bond by a more labile ester bond. However, a minimum detrimental effect was expected due to the crowded environment of such a group in the final material.

Reversible Addition-Fragmentation Chain-Transfer Polymerization (RAFT) Polymerization of Acrylic Monomers In order to build a bifunctional acrylic polymer (**P1**), the synthetized monomers **M1** and **M2** were polymerized with *N*,*N*-dimethyl acrylamide as structural monomer (**M3**). The structural heterogeneity of the three monomers suggested a living radical polymerization strategy. Specifically, RAFT using *S*-1-dodecyl-*S*′-(*α*,*α*-dimethyl-*α*″-acetic acid)trithiocarbonate (DDMAT) as RAFT agent was considered the most suitable strategy to obtain the desired polymer with low dispersity. Thus, polymerization of monomers **M1**–**M3** in a molar ratio of 1 : 1 : 8 was performed as previously reported,[22] with changes in the monomer with disulfide functionality (**M2**), which in this work was an acrylate instead of an acrylamide, to obtain the desired polymer **P1**. Size exclusion chromatography analysis (SEC) of **P1** afforded one peak with an average molecular weight (M_w) of 12500 g/mol and a polydispersity index of 2.3. NMR analysis displayed signals characteristic of each monomer, however, the lack of vinylic signals strongly suggested the absence of free monomeric units. The proportion of monomers in the copolymer can be roughly determined by comparing the integral ratios of the aldehyde protons of **M1**, the aromatic protons of **M2** and the $N(CH_3)_2$ protons of

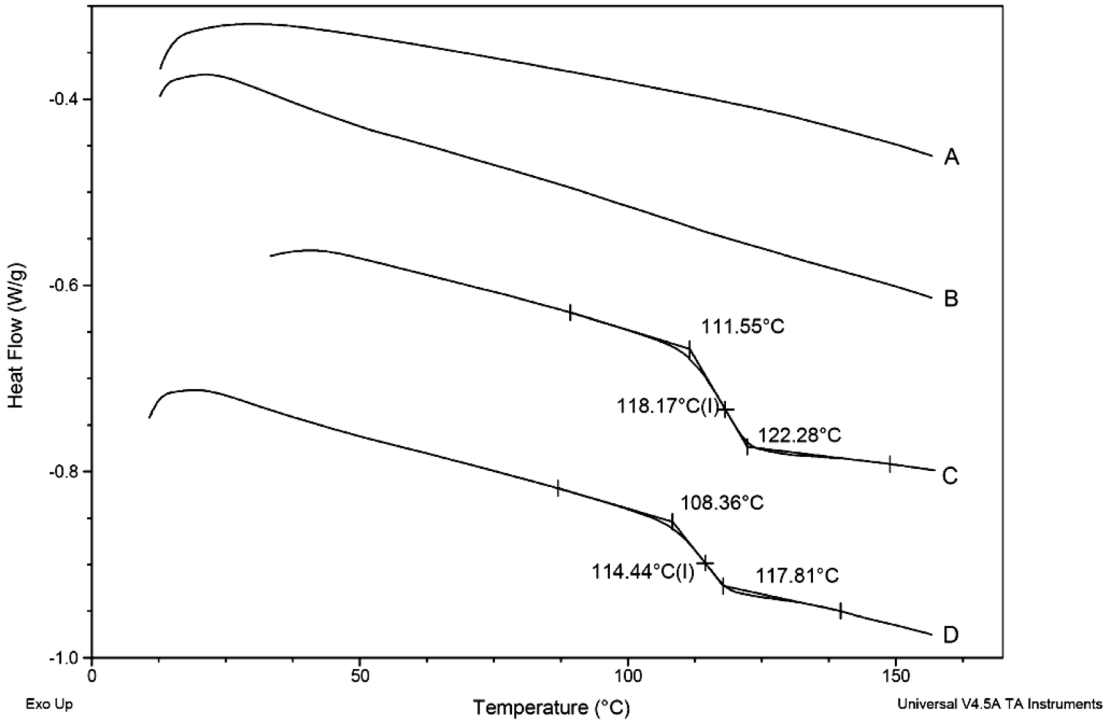

Fig. 4. DSC Profiles of Different Nanoparticles

(A) Stimuli sensitive nanoparticles, (B) thiolated chitosan nanoparticles, (C) acrylic polymer nanoparticles, (D) mixture of thiolated chitosan nanoparticles and acrylic polymer nanoparticles.

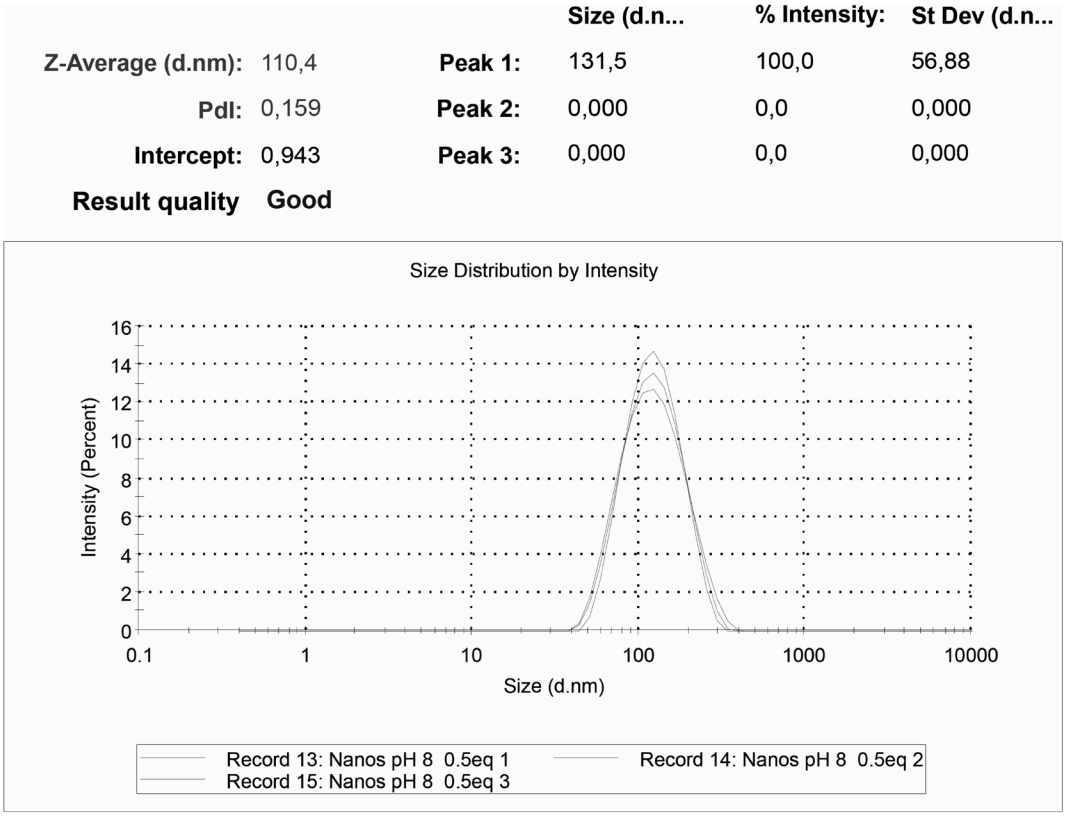

Fig. 5. Particle Size of Polymer Nanoparticles Functionalized with PEG 5000 NHS

M3. The monomer composition was determined to be 12 : 1 : 1 (**M3** : **M1** : **M2**) which differs to the feed ratio, presumably due to the difference in reactivity between the monomers and or incomplete polymerization.

A comparative differential scanning calorimetry analysis (DSC) of **P1** against homopolymers of **M1** and **M3** and copo-

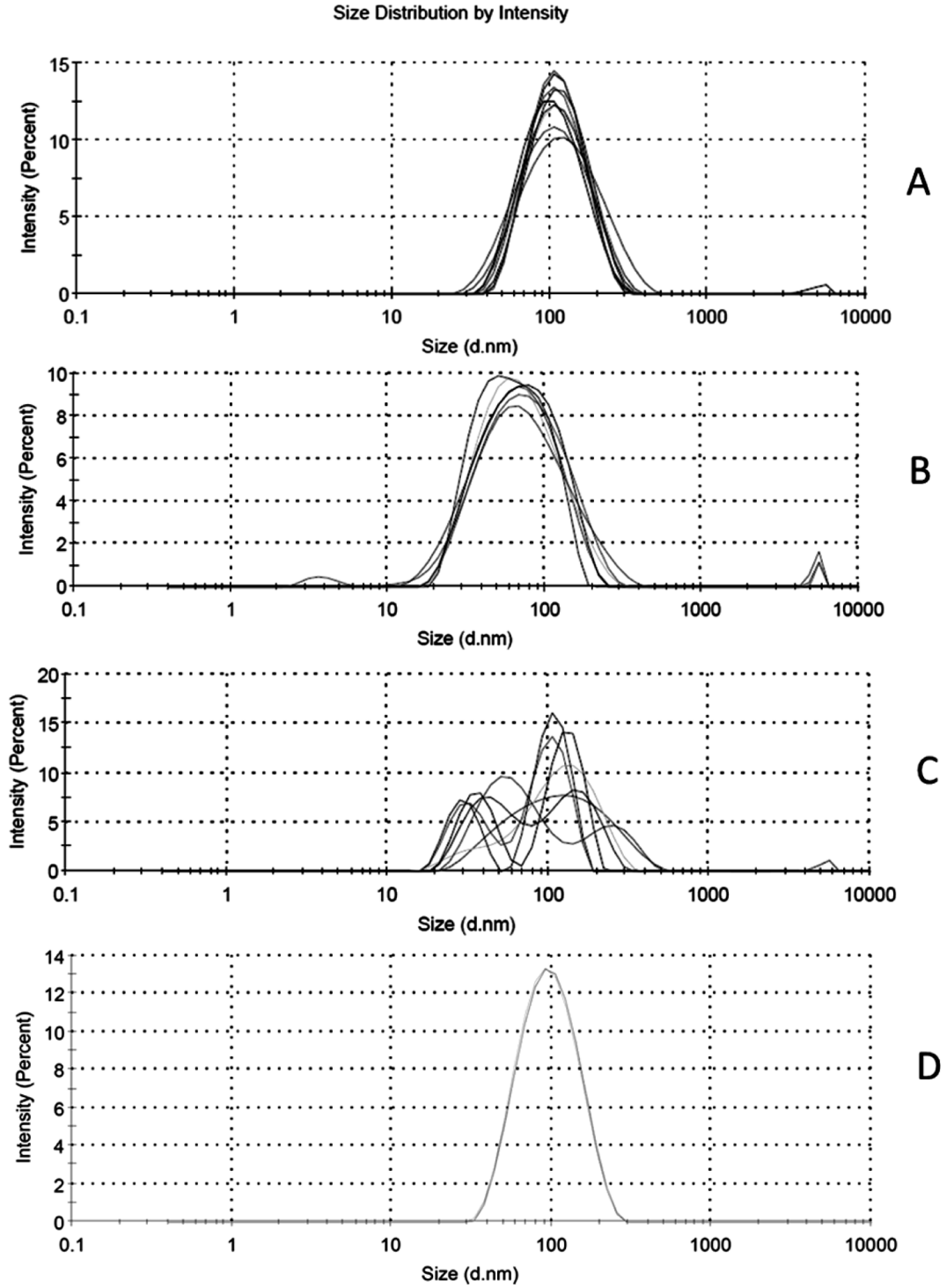

(A) pH 5.5 without TCEP. (B) TCEP+pH 8.0. (C) TCEP+pH 5.5. (D) Polymer nanoparticles without treatment.

Chart 4. Particle Size Distribution of Polymer Nanoparticles under Different Environments

lymers of **M2** and **M3** (50 : 50 ratio) can be seen in Fig. 1. An homopolymer of **M2** could not be obtained despite literature reports.[45)]

The homopolymer of **M3**, exhibited an endothermic event at 110°C in agreement with the glass transition temperature (T_g) reported in the literature.[46)] Interestingly, the homopolymer of **M1**, presented a T_g at 100°C, which is quite close to the value found for **P1** (T_g 101°C) despite the fact that the molar ratio composition of **P1** is 12 : 1 : 1 (**M3** : **M1** : **M2**). These results indicate a higher flexibility in the **P1** copolymer due to the incorporation of more bulky monomers **M1** and **M2** in comparison to homopolymer of PDMA (**M3**). It is worth to mention that only one T_g signal is observed in **P1**, which suggest an adequate copolymerization of the monomers. The thermal behavior of the copolymer made with **M2** and **M3**, depicts two successive T_g events, one at 84°C and the second at 103°C. These results indicate that **M2** decrease the T_g of the polymer when it is copolymerized with **M3**. In general these

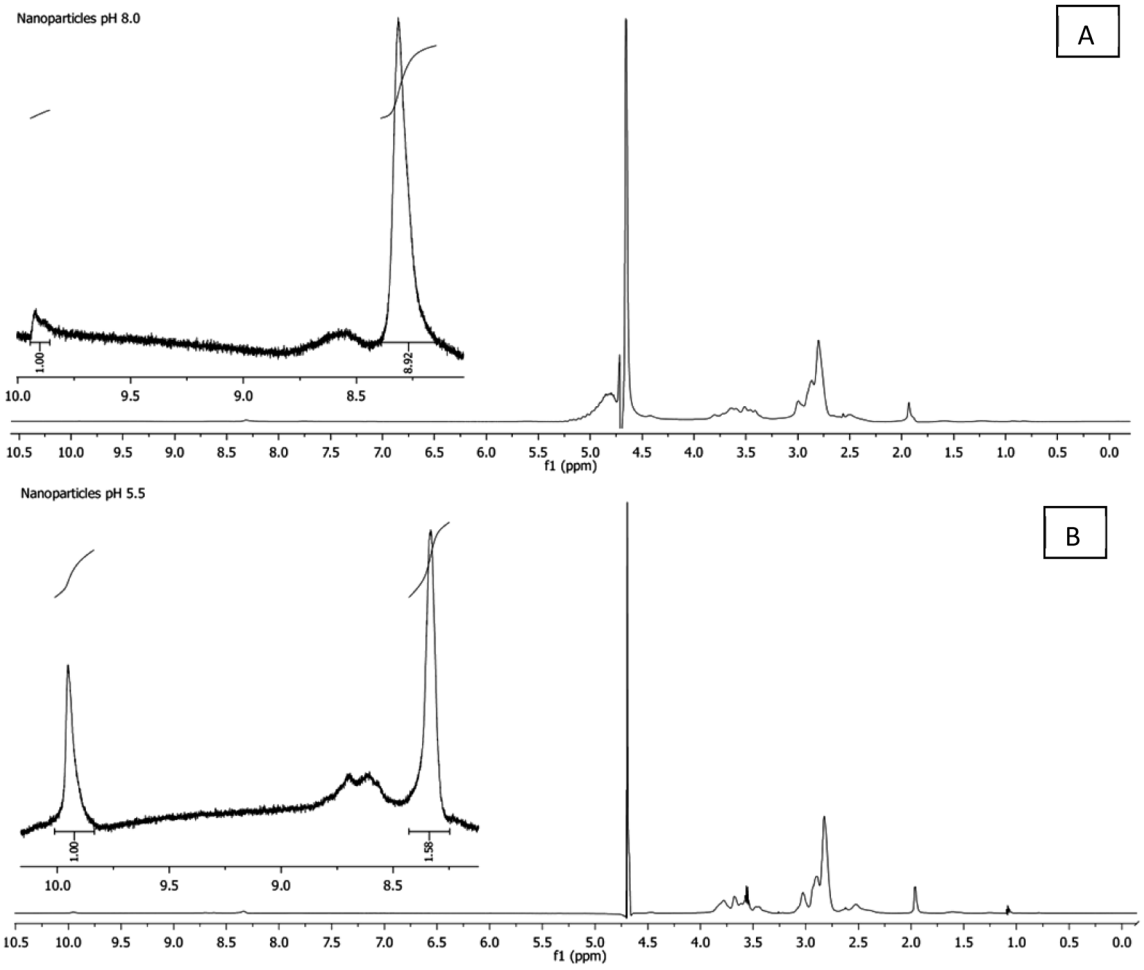

(A) pH 8.0; (B) pH 5.5.

Chart 5. ^{1}H-NMR Spectrum of Stimuli Sensitive Polymer Nanoparticles at Different pH

analysis suggest that the thermal behavior of **P1** is the result of the interaction of three different monomers in which the effect of the major component (**M3**) imparts the brittleness property while **M1** and **M2** exert a plasticizer effect.

Chitosan Hydrolysis and Functionalization In order to obtain low size chitosan particles, it was necessary to submit the polymer to partial hydrolysis with sodium nitrite. Further functionalization by means of thioglycolic acid esterification mediated by EDC afforded a polymer, sensitive to redox potential, with a viscosity average molecular weight (M_v, according to the Mark–Houwink equation) of 12300 g/mol. Similar molecular weights have been reported as suitable to make chitosan nanoparticles with sizes between 100 and 200 nm.[47,48] The degree of functionalization with thiol groups was assessed with Ellman's reagent and the result found was 290 μmol/g of functionalized polymer which means that *ca.* 6% of the primary amine groups of the chitosan chain were functionalized. Comparable results were reported when chitosan was functionalized with 2-iminothiolane or thioglycolic acid.[49,50] ^{1}H-NMR analysis confirm a change in the chemical environment for the hydrogen linked to the anomeric carbon (C-1) of the glucosamine units, and the hydrogen linked next to it (C-2). This suggests that functionalization took place over the primary amine bonded to C-2. These results were also confirmed by HSQC and HMBC analysis available in the Supplementary Material.

Stimuli Sensitive Polymer Nanoparticles Final cross-linked polymer nanoparticles were made using different proportions of polymers; however, the size of nanoparticles made with 50% of the acrylic polymer (**P1**) and 50% of thiolated chitosan showed the lowest polydispersity index (PDI) (0.158) in which a single peak that represent 100% of the intensity with a mean particle size of 103 nm was observed (Fig. 2). To confirm the results found by DLS and to know the morphology of the nanoparticles, transmission electron microscopy (TEM) analysis was conducted using uranyl acetate as contrast agent. Figure 3 shows spherical nanoparticles with sizes around 90 nm, which are in agreement with the range of sizes found by DLS. As has been reported in several reviews and research articles, particle size is a parameter with high relevance in many fields, but especially in nanomedicine where particles are going to be used as drug delivery systems, because they will be easily detected and degraded by the mononuclear phagocytic system (MPS) when the particles have a size higher than 200 nm.[51] On the other hand, if the particles have a size smaller than 10 nm, they can be removed from the circulation by glomerular filtration.[52] In our case, DLS and TEM analysis confirm the suitability of the synthesized particles in terms of size. Another important aspect to consider in the development of drug carriers is the *Z* potential, since high positive or negative charges can be detected as well by the MPS.[53] The *Z* potential observed was around +2 mV for the

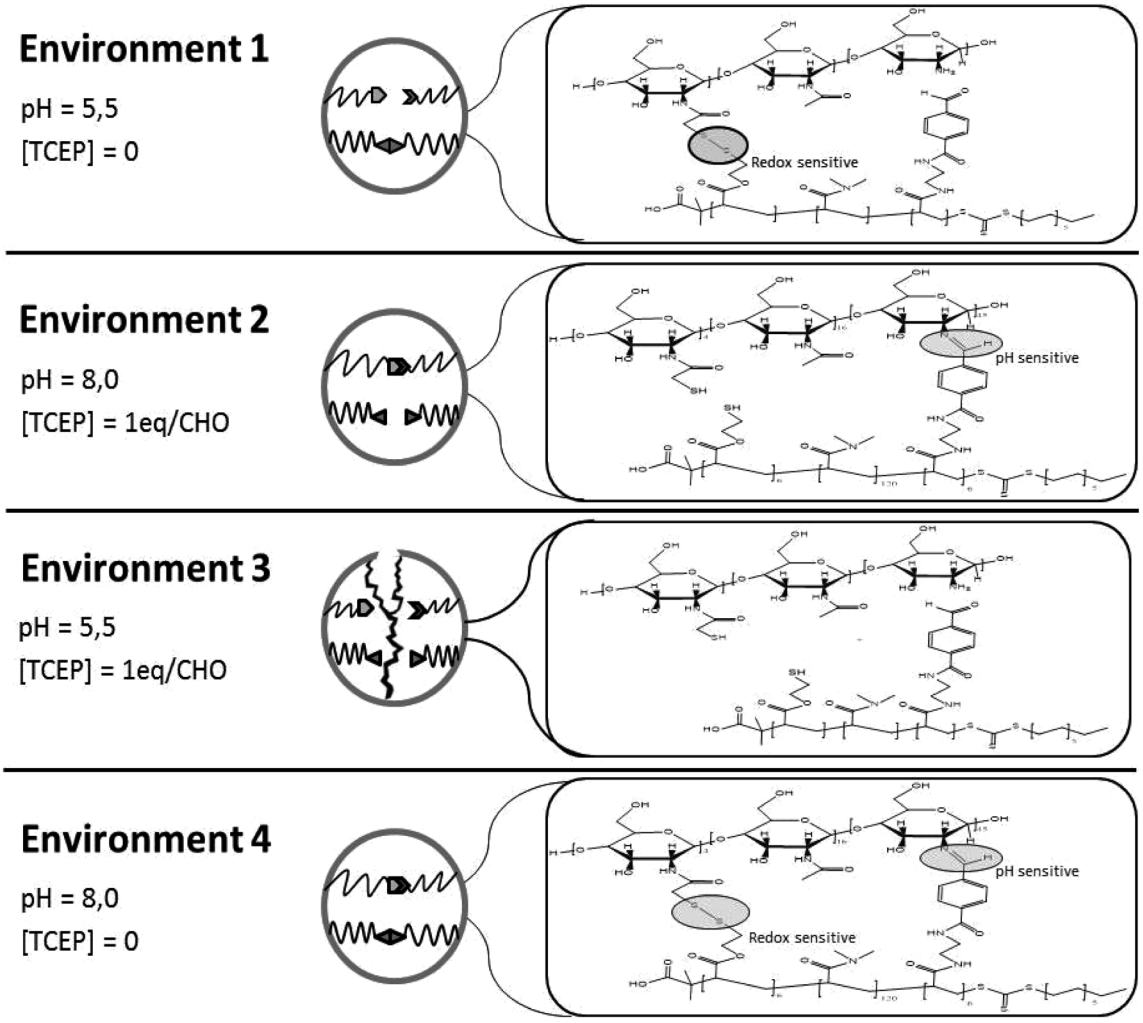

Chart 6. Schematic Behavior of Stimuli Sensitive Polymer Nanoparticles in 4 Different Environments

cross-linked polymer nanoparticles. This level of charge on the particles surface makes them less immunogenic and therefore potentially suitable for drug delivery. In order to assess the linkage between the acrylic polymer (**P1**) and the thiolated chitosan, thermal analysis by DSC was conducted. For this goal, a comparative thermal behavior analysis of acrylic polymer nanoparticles, thiolated chitosan nanoparticles, a physical mixture of acrylic polymer nanoparticles and thiolated chitosan nanoparticles, and the final assembled stimuli sensitive nanoparticles (cross-linked) was conducted. Nanoparticles instead of polymers were used in order to discard any change in the thermal behavior induced by the nanoparticles preparation method. The results, shown in Fig. 4, display a T_g event at 118°C for the acrylic nanoparticles and a T_g event at 114°C for the physical mixture of acrylic nanoparticles and thiolated chitosan nanoparticles. However, the thiolated chitosan nanoparticles and the stimuli sensitive nanoparticles did not present any thermal event. This fact indicates that there was a strong interaction between the chemical groups of **P1** and thiolated chitosan with the generation of a new polymeric structure with greater stiffness between the chains due to favorable intermolecular interactions. This is in agreement with the curing or crosslinking processes between polymeric chains where the T_g temperature of the new polymeric material can increase or even disappear of the range of analysis generally due to restriction on main-chain motion by the crosslinks.[54,55] Another reason that supports the disappearance of the T_g in the thermal behavior of the stimuli sensitive nanoparticles, is the random interconnection between the polymers which does not allow a movement pattern in the backbone of the polymer as a product of the heating and makes the measure of the T_g truly difficult.[56]

Functionalization of Polymer Nanoparticles The stability of colloidal systems can be considered a drawback in the development of drug delivery systems. It is commonly accepted that colloidal systems with a Z potential between +30 and −30 mV could be very unstable.[57,58] Considering that our stimuli sensitive polymer nanoparticles possess a charge in that range, it was deemed necessary to functionalize the surface of the nanoparticles with a hydrophilic polymer. For this aim PEG functionalization was considered the most suitable option. Additionally pegylation was done thinking in long-term stability of the nanoparticles in biological media when they will be used *in-vivo*. Is well known that PEG increases the circulation time in blood because PEG reduces a fast clearance of the nanoparticles and hence improves efficiency by enhanced permeability and retention effect. PEG has been extensively used to increase surface hidrophilicity and improve circulation half-life by decreasing interactions with blood proteins and MPS cells.[59–62]

In this work PEGylation was conducted by covalently attaching PEG chains onto the surface of nanoparticles, a preactivated PEG was used (PEG-NHS). *N*-Hydroxylsuccinimide (NHS) functionalized polyethylene glycol (PEG-NHS) is an amino ($-NH_2$) reactive PEG derivatives that can be used to modify protein, peptide or any other surfaces with available amino groups, such as the stimuli-sensitive nanoparticles surface due to chitosan chains. NHS esters react with primary amine groups to form stable amide bonds. Compared to other NHS ester, succinimidyl carbonate linker provides much higher stability in aqueous solution with good yield in the coupling reaction.[63–65]

The new PEG functionalized particles displayed one peak with an average particle size of 131 nm as measured by DLS. This is 30 nm higher than the non-functionalized nanoparticles (Figs. 2, 5). An increase of the *Z* potential up to +10 mV and an improvement in the colloidal stability was also experimented after the functionalization process with PEG.

Stimuli Sensitive Assessment The polymer carrier developed in this work was designed with the intention of being disassembled under pH and redox potential conditions commonly found in cancer cells.[66,67] This ability was assessed in four different environments and monitored by DLS using the particle size and the PDI as indicators of disassembly or disintegration of the particles. The first environment assessed was basically water with a pH value of 5.5. This environment applies only to the pH stimuli and has as target the imine bond that was formed by the coupling of the aldehyde groups present in the pendant chains of the acrylic polymer (**P1**) and the primary amine groups available in the thiolated chitosan. Imines are accepted to be stable at normal physiological pH values but can be easily broken at pH values around 5.5 which are pH values commonly found in cancer cells.[66,68] DLS analysis showed one peak with an average particle size of 136 nm and a PDI of 0.216 as is depicted in Chart 4A. In addition, NMR analysis (Chart 5) of the integral ratio between imine signals around 8.2–8.4 ppm and aldehydes around 10 ppm for the control (A) and pH stimuli sensitive nanoparticle (B) revealed significant changes in favor of an increase of aldehyde groups when the pH changes from 8.0 to 5.5. This result indicates an expansion of the particle size probably as a consequence of imine breaking, which is one of the bonds that allow the integration between **P1** and thiolated chitosan. In the second environment, the target was the disulfide bonds product of the reaction between thiols groups from **P1** and thiolate chitosan, pH was kept at a value of 8.0, which is the original pH of the nanoparticles (non pH stimulus), and the effect of changing the redox potential by means of tris(2-carboxyethyl)phosphine hydrochloride (TCEP) addition was measured. TCEP is an effective reagent for the cleavage of disulfide bonds in aqueous solution.[69] The particle size distribution found in this second environment depicts a wide peak with a particle size of 85 nm, which represents a small contraction of the original particle size as seen in Chart 4B. A third environment was assessed in which both stimuli were applied at the same time with hard effects in the nanoparticle structure as shown in Chart 4C. Several random populations were evidenced which could be interpreted as the final result of the simultaneous breaking of the imine and disulfide bonds which suggest the separation of the structural polymers of the nanoparticles. The last environment was a control were neither pH nor redox potential stimuli were applied, therefore non change was found (Chart 4D). A schematic representation that summarizes the structural changes undergone by the stimuli sensitive nanoparticles as a result of the exposition to specific environments is depicted in Chart 6.

Conclusion

In the present work, polymeric nanoparticles with sizes around 100 nm were obtained by means of the cross-linking between low molecular weight thiolated chitosan and a bifunctional acrylic copolymer (**P1**) using imines and disulfides as dynamic covalent bonds. The particles were able to keep their structure when single pH or redox stimuli were applied. However, simultaneous application of both stimuli resulted in disassembly of the macrostructure. These stimuli sensitive polymer nanoparticles can be considered a promising alternative to deliver an active substance in a desired environment.

Acknowledgments This work was financially supported by Universidad de Antioquia, COLCIENCIAS (scholarship 567-2012) and Institut Galien Paris-Sud UMR CNRS 8612.

Conflict of Interest The authors declare no conflict of interest.

Supplementary Materials The online version of this article contains supplementary materials.

References

1) Rosen H., Abribat T., *Nat. Rev. Drug Discov.*, **4**, 381–385 (2005).
2) Yatvin M. B., Weinstein J. N., Dennis W. H., Blumenthal R., *Science*, **202**, 1290–1293 (1978).
3) Marslin G., Sheeba C. J., Kalaichelvan V. K., Manavalan R., Reddy P. N., Franklin G., *J Biomed Nanotechnol*, **5**, 464–471 (2009).
4) Matsumoto A., Matsukawa Y., Suzuki T., Yoshino H., *J. Control. Release*, **106**, 172–180 (2005).
5) Nishiyama N., Okazaki S., Cabral H., Miyamoto M., Kato Y., Sugiyama Y., Nishio K., Matsumura Y., Kataoka K., *Cancer Res.*, **63**, 8977–8983 (2003).
6) Mora-Huertas C. E., Fessi H., Elaissari A., *Int. J. Pharm.*, **385**, 113–142 (2010).
7) Veiseh O., Gunn J. W., Zhang M., *Adv. Drug Deliv. Rev.*, **62**, 284–304 (2010).
8) Patra C. R., Bhattacharya R., Mukhopadhyay D., Mukherjee P., *Adv. Drug Deliv. Rev.*, **62**, 346–361 (2010).
9) Goutayer M., Dufort S., Josserand V., Royère A., Heinrich E., Vinet F., Bibette J., Coll J.-L., Texier I., *Eur. J. Pharm. Biopharm.*, **75**, 137–147 (2010).
10) Mahmoudi M., Sant S., Wang B., Laurent S., Sen T., *Adv. Drug Deliv. Rev.*, **63**, 24–46 (2011).
11) Reid Y. A., "Characterization and Authentication of Cancer Cell Lines: An Overview," Humana Press, Totowa, NJ, 2011, pp. 35–43.
12) Janku F., *Therapeutic Advances in Medical Oncology*, **6**, 43–51 (2014).
13) Mura S., Nicolas J., Couvreur P., *Nat. Mater.*, **12**, 991–1003 (2013).
14) Torchilin V. P., *Nat. Rev. Drug Discov.*, **13**, 813–827 (2014).
15) Zhu, L., Torchilin, V. P., *Integrative Biology: quantitative biosciences from nano to macro*, **5**, 96–107 (2013).
16) Torchilin V., *Eur. J. Pharm. Biopharm.*, **71**, 431–444 (2009).
17) de la Torre P. M., Torrado G., Torrado S., *J. Biomed. Mater. Res. B Appl. Biomater.*, **72**, 191–197 (2005).
18) Rowan S. J., Cantrill S. J., Cousins G. R. L., Sanders J. K. M., Stoddart J. F., *Angew. Chem. Int. Ed.*, **41**, 898–952 (2002).
19) Jackson A. W., Fulton D. A., *Polymer Chemistry*, **4**, 31–45 (2013).

20) Godoy-Alcántar C., Yatsimirsky A. K., Lehn J. M., *J. Phys. Org. Chem.*, **18**, 979–985 (2005).
21) Bapat A. P., Ray J. G., Savin D. A., Sumerlin B. S., *Macromolecules*, **46**, 2188–2198 (2013).
22) Jackson A. W., Fulton D. A., *Macromolecules*, **45**, 2699–2708 (2012).
23) Wang Y., Zhao Q., Han N., Bai L., Li J., Liu J., Che E., Hu L., Zhang Q., Jiang T., Wang S., *Nanomedicine*, **11**, 313–327 (2015).
24) Gaber M., Medhat W., Hany M., Saher N., Fang J.-Y., Elzoghby A., *J. Control. Release*, **254**, 75–91 (2017).
25) Jiang X.-C., Gao J.-Q., *Int. J. Pharm.*, **521**, 167–175 (2017).
26) Periayah M. H., Halim A. S., Saad A. Z. M., *Pharmacognosy Reviews*, **10**, 39–42 (2016).
27) Elgadir M. A., Uddin M. S., Ferdosh S., Adam A., Chowdhury A. J. K., Sarker M. Z. I., *Journal of Food and Drug Analysis*, **23**, 619–629 (2015).
28) Cira L. A., Huerta S., Hall G. M., Shirai K., *Process Biochem.*, **37**, 1359–1366 (2002).
29) Beaney P., Lizardi-Mendoza J., Healy M., *J. Chem. Technol. Biotechnol.*, **80**, 145–150 (2005).
30) Hirano S., Seino H., Akiyama Y., Nonaka I., "Chitosan: A Biocompatible Material for Oral and Intravenous Administrations," Springer US, Boston, MA, 1990, pp. 283–290.
31) Thorat N. D., Otari S. V., Patil R. M., Bohara R. A., Yadav H. M., Koli V. B., Chaurasia A. K., Ningthoujam R. S., *Dalton Trans.*, **43**, 17343–17351 (2014).
32) Dash M., Chiellini F., Ottenbrite R. M., Chiellini E., *Prog. Polym. Sci.*, **36**, 981–1014 (2011).
33) Croisier F., Jérôme C., *Eur. Polym. J.*, **49**, 780–792 (2013).
34) Xia W., Liu P., Zhang J., Chen J., *Food Hydrocoll.*, **25**, 170–179 (2011).
35) Benhabiles M. S., Salah R., Lounici H., Drouiche N., Goosen M. F. A., Mameri N., *Food Hydrocoll.*, **29**, 48–56 (2012).
36) Leithner K., Bernkop-Schnürch A., "Chitosan and Derivatives for Biopharmaceutical Use: Mucoadhesive Properties," John Wiley & Sons, Ltd., 2012, pp. 159–180.
37) El-Hefian E. A., Nasef M. M., Yahaya A. H., *J. Chem. Soc. Pak.*, **36**, 11–27 (2014).
38) Sionkowska A., *Prog. Polym. Sci.*, **36**, 1254–1276 (2011).
39) Crosby I. T., Pietersz G. A., Ripper J. A., *Aust. J. Chem.*, **61**, 138–143 (2008).
40) Ghosh S., Basu S., Thayumanavan S., *Macromolecules*, **39**, 5595–5597 (2006).
41) Bulmus V., Woodward M., Lin L., Murthy N., Stayton P., Hoffman A., *J. Control. Release*, **93**, 105–120 (2003).
42) Seong H.-S., Kim J.-P., Ko S.-W., *Text. Res. J.*, **69**, 483–488 (1999).
43) Kasaai M. R., Arul J., Charlet G., *J. Polym. Sci., B, Polym. Phys.*, **38**, 2591–2598 (2000).
44) Iqbal J., Shahnaz G., Perera G., Hintzen F., Sarti F., Bernkop-Schnürch A., *Eur. J. Pharm. Biopharm.*, **80**, 95–102 (2012).
45) Remant B. K., Chandrashekaran V., Cheng B., Chen H., Peña M. M., Zhang J., Montgomery J., Xu P., *Mol. Pharm.*, **11**, 1897–1905 (2014).
46) Hadj Hamou A. S., Djadoun S., *Macromol. Symp.*, **303**, 114–122 (2011).
47) Chattopadhyay, D. P., Inamdar, M. S., *Research Journal of Engineering Sciences*, **1**, 9–15 (2012).
48) Ing L. Y., Zin N. M., Sarwar A., Katas H., *Int. J. Biomater.*, **2012**, 9 (2012).
49) Kast C. E., Bernkop-Schnürch A., *Biomaterials*, **22**, 2345–2352 (2001).
50) Schmitz T., Bravo-Osuna I., Vauthier C., Ponchel G., Loretz B., Bernkop-Schnürch A., *Biomaterials*, **28**, 524–531 (2007).
51) Kulkarni S. A., Feng S.-S., *Pharm. Res.*, **30**, 2512–2522 (2013).
52) Choi C. H. J., Zuckerman J. E., Webster P., Davis M. E., *Proc. Natl. Acad. Sci. U.S.A.*, **108**, 6656–6661 (2011).
53) Poznansky M. J., Juliano R. L., *Pharmacol. Rev.*, **36**, 277–336 (1984).
54) Kessler M. R., White S. R., *J. Polym. Sci. A Polym. Chem.*, **40**, 2373–2383 (2002).
55) Wu Y.-H., Freeman B. D., *J. Membr. Sci.*, **344**, 182–189 (2009).
56) Hatakeyama, T., Quinn, F. X., "Thermal Analysis: Fundamentals and Applications to Polymer Science," 1999, pp. 90–91.
57) Riddick T. M., "Control of colloid stability through zeta potential: with a closing chapter on its relationship to cardiovascular disease," Published for Zeta-Meter, Inc., by Livingston Pub. Co., New York, 1968, p. 372.
58) Honary S., Zahir F., *Trop. J. Pharm. Res.*, **12**, 265–273 (2013).
59) Bazile D., Prud'homme C., Bassoullet M. T., Marlard M., Spenlehauer G., Veillard M., *J. Pharm. Sci.*, **84**, 493–498 (1995).
60) Fang C., Bhattarai N., Sun C., Zhang M., *Small*, **5**, 1637–1641 (2009).
61) Saei A. A., Yazdani M., Lohse S. E., Bakhtiary Z., Serpooshan V., Ghavami M., Asadian M., Mashaghi S., Dreaden E. C., Mashaghi A., Mahmoudi M., *Chem. Mater.*, **29**, 6578–6595 (2017).
62) Barenholz Y., *J. Control. Release*, **160**, 117–134 (2012).
63) Perry J. L., Reuter K. G., Kai M. P., Herlihy K. P., Jones S. W., Luft J. C., Napier M., Bear J. E., DeSimone J. M., *Nano Lett.*, **12**, 5304–5310 (2012).
64) Bailon P., Won C.-Y., *Expert Opin. Drug Deliv.*, **6**, 1–16 (2009).
65) Fee C. J., Van Alstine J. M., *Chem. Eng. Sci.*, **61**, 924–939 (2006).
66) Tannock I. F., Rotin D., *Cancer Res.*, **49**, 4373–4384 (1989).
67) Ortega A. L., Mena S., Estrela J. M., *Cancers*, **3**, 1285–1310 (2011).
68) Layer R. W., *Chem. Rev.*, **63**, 489–510 (1963).
69) Burns J. A., Butler J. C., Moran J., Whitesides G. M., *J. Org. Chem.*, **56**, 2648–2650 (1991).